Degradation of phosphorene in air: understanding at atomic level

2D Materials

PAPER

Degradation of phosphorene in air: understanding at atomic level

Gaoxue Wang[1], William J Slough[1], Ravindra Pandey[1] and Shashi P Karna[2]

1   Department of Physics, Michigan Technological University, Houghton, MI 49931, USA
2   US Army Research Laboratory, Weapons and Materials Research Directorate, ATTN: RDRL-WM, Aberdeen Proving Ground, MD 21005-5069, USA
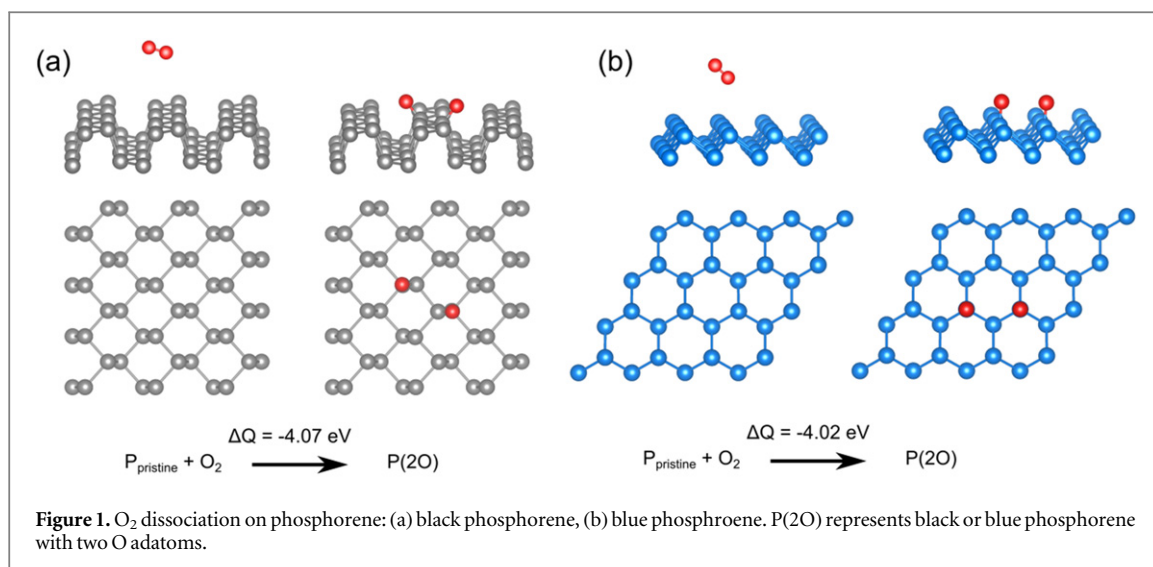
E-mail: pandey@mtu.edu

Abstract

Phosphorene is a promising two-dimensional (2D) material with a direct band gap, high carrier mobility, and anisotropic electronic properties. Phosphorene-based electronic devices, however, are found to degrade upon exposure to air. In this paper, we provide an atomic level understanding of the stability of phosphorene in terms of its interaction with O_2 and H_2O. The results based on density functional theory together with first principles molecular dynamics calculations show that O_2 could the spontaneously dissociate on phosphorene at room temperature. H_2O will not strongly interact with pristine phosphorene, however, an exothermic reaction could occur if phosphorene is first oxidized. The pathway of oxidation first, followed by exothermic reaction with water is the most likely route for the chemical degradation of phosphorene-based devices in air.

1. Introduction

Phosphorene is one of the group V elemental monolayers [1–4] with a direct band gap, high carrier mobility, and anisotropic electronic properties, making it a promising candidate for applications in electronics and optoelectronics [5, 6]. The chemical degradation of phosphorene upon exposure to ambient conditions, however, is a challenge to the stability and performance of phosphorene-based devices [7–11]. The presence of oxygen and humidity is suggested to be the main cause of the degradation process [12–14]. Recent experiments have also demonstrated photo-assisted degradation of phosphorene [15], which is predicted to be related to intrinsic defects [16]. Theoretically, it was reported that H_2O adsorbed on phosphorene will induce a significant distortion to its structure [8]. Contradictory results were obtained suggesting that phosphorene is stable in the presence of H_2O [17]. Despite these experimental and theoretical efforts, there are still some unanswered questions regarding the degradation of phosphorene, including (i) atomic level of understanding on the degradation process of phosphorene; (ii) the role of H_2O in the degradation process; and (3) the

environmental stability of other theoretically predicted phosphorene allotropes (e.g., blue phosphorene [18] which has not been realized in experiments).

In order to address these questions, we have performed density functional theory (DFT) calculations combined with first principles molecular dynamics (MD) simulations to investigate the interactions of O_2 and H_2O with phosphorene. In section 3.1, we focus on the interaction of O_2 with phosphorene. Since surface reaction with O_2 has been reported to be crucial in the degradation process of black phosphorene [14], we will extend the discussion to blue phosphorene. In section 3.2, the adsorption of H_2O on phosphorene allotropes is investigated in terms of adsorption configuration, binding energy, and bonding characteristics. In section 3.3, we discuss the degradation of phosphorene by calculating the relative energies along a likely interaction pathway. Our calculated results show that O_2 can spontaneously dissociate on phosphorene at room temperature. H_2O will not strongly interact with pristine phosphorene, however, an exothermic reaction could occur if phosphorene is first oxidized. Other allotropes of phosphorene, e.g. blue phosphorene are also expected to deteriorate in air.

Figure 1. O_2 dissociation on phosphorene: (a) black phosphorene, (b) blue phosphroene. P(2O) represents black or blue phosphorene with two O adatoms.

2. Computational details

The electronic structure calculations were performed using the Vienna *ab initio* simulation package [19, 20]. The exchange-correlation was treated within the generalized gradient approximation (GGA) using Perdew−Burke−Ernzerhof (PBE) [21] functional for the calculations. We also employed the DFT-D2 method of Grimme [22] to include contributions from the van der Waals (vdW) interactions. The energy of convergence was set to 1×10^{-6} eV and the residual force on each atom was smaller than 0.01 eV Å^{-1} during the structural optimization. The cutoff energy for the plane-wave basis was set to 500 eV. The vacuum distance normal to the plane was larger than 30 Å to eliminate interaction between the periodic replicas. A rectangular supercell of (3×4) was used for the black phosphorene, and a parallelogram supercell of (4×4) was used for the blue phosphorene. The reciprocal space was sampled by a grid of $(2 \times 2 \times 1)$ k points in the Brillouin Zone.

First principles MD simulations were also performed to simulate the interaction processes considered. The MD simulation was based on the norm-conserving Troullier-Martins pseudopotential together with Nosé thermostat [23] as implemented in the SIESTA program package [24]. In order to minimize the constraints induced by periodicity in the slab model for MD simulations, (5×6) and (5×5) supercells were used for black and blue phosphorene, respectively. The time step was set to 1 fs, and the simulation temperature was set to 300 K. It is to be noted that most of the experiments on degradation of phosphorene were done in the air. In our MD simulations, the number density of gas molecules was about 65.8×10^{25} m^{-3} considering 9 O_2 molecules in a simulation cell of $(22.9$ Å $\times 19.9$ Å $\times 30$ Å$)$. Such high pressure conditions were also used for MD simulations to study oxidation of SiC [25] and graphene [26].

3. Results and discussion

Black phosphorene has a puckered surface with two sub-layers of phosphorus atoms which are arranged in a rectangular lattice. At GGA-PBE level of theory, the lattice constants along the armchair and the zigzag direction are 4.57 Å and 3.31 Å, respectively. The bond lengths are 2.22 Å and 2.25 Å. Blue phosphorene has a buckled honeycomb structure with lattice constant of 3.28 Å and bond length of 2.26 Å. Our results are in agreement with the reported lattice constants and bond lengths of black and blue phosphorene [2, 18], thereby, demonstrating the reliability of the modeling elements used in the calculations.

3.1. O_2 interacting with phosphorene

It has been established by both calculations and experiments that O_2 can easily dissociate on black phosphorene [14, 27] leading to the formation of the oxidized lattice [28]. The O_2 molecule prefers a perpendicular configuration to approach the surface of phosphorene with a distance of 2.5 Å as seen from the binding energy profile (figure S1 in the supplementary materials). Thereafter, O_2 tends to dissociate on the surface with exothermic energy (ΔQ) of -4.07 eV/O_2 molecule on black phosphorene, and -4.02 eV/O_2 molecule on blue phosphorene (figure 1). The details of calculations for ΔQ are given in table S1 in the supplementary materials. Note that the dissociation energy is calculated using the triplet state of O_2.

The calculated dissociation barrier of O_2 on phosphorene is 0.54 eV [14]. Considering that chemical reaction with an energy barrier less than 0.9 eV $(\approx 21$ kcal mol$^{-1})$ from DFT calculations could occur at room temperature [29], oxidation of phosphorene is expected to occur readily at room temperature. Other external sources such as photon radiation may speed up the dissociation process. After dissociation, atomic oxygen finds the dangling position to be the

Table 1. Structural properties of atomic O adsorbed on phosphorene.

Phosphorene	Black	Blue
Bond length R_{P-O} (Å)	1.50 Å	1.50 Å
Bond angle $\angle P-P-O$ (°)	112°, 117°	123°
Bader charge, oxygen	−1.31e	−1.32e

preferred site on black phosphorene which is consistent with previous theoretical studies [14, 28, 30]. This is not the case with blue phosphorene where the preferred site is the top site (see figure S2 in the supplementary materials). The P–O bond shows similar bonding character as seen from the bond length and Bader charges [31] given in table 1. Overall, the nature of interaction of oxygen with phosphorene stems from the sp^3 bonds which leave a lone electron pair on each phosphorous atom, and the preferred binding site follows the direction of the lone electron pair on both allotropes.

The calculated results based on first principles MD simulations further affirm the dissociation of O_2 on phosphorene. Figure 2 shows time-dependent snapshots of the configurations showing interaction of oxygen with phosphorene during MD simulations. These configurations were obtained by placing a few O_2 molecules 4 Å initially above the surface at a constant temperature of 300 K. For the case of black phosphorene, some O_2 molecules will first move closer to the native phosphorus atoms, then dissociate into atomic oxygen atoms after 600 fs (see video V1 in the supplementary materials). A similar O_2 dissociation process is seen on the blue phosphorene after 1150 fs (see video V2 in the supplementary materials).

Considering the relatively high pressure conditions in our MD simulations, we have performed additional MD calculations with only one O_2 molecule in the simulation box of (22.9 Å × 19.9 Å × 85 Å) which appears to mimic number density of gas molecules of 2.5×10^{25} m^{-3} under standard atmospheric conditions. The results shown in figure S3, video V3 and video V4 (supplementary materials) find that dissociation of O_2 on the surface does occur under the relatively reduced pressure conditions. We may therefore conclude that both allotropes of phosphorene will go through the spontaneous oxidation process upon exposure to O_2 at room temperature due to the affinity of P and O atoms forming P=O bonds with a large exothermic energy (see figure 1).

3.2. H_2O interacting with phosphorene

Figure 3 shows the configurations of H_2O interacting with phosphorene considered for the calculations: one leg, two leg, and O closer. The configuration referred to as 'one leg' is the configuration in which one of the H atoms is closer to the surface, 'two leg' means both H atoms are closer to the surface, and 'O closer' means the O atom is closer to the surface.

The calculated binding energy profiles with vdW correction using DFT-D2 method of Grimme [22] are shown in figure 4. Some of the results deduced are:
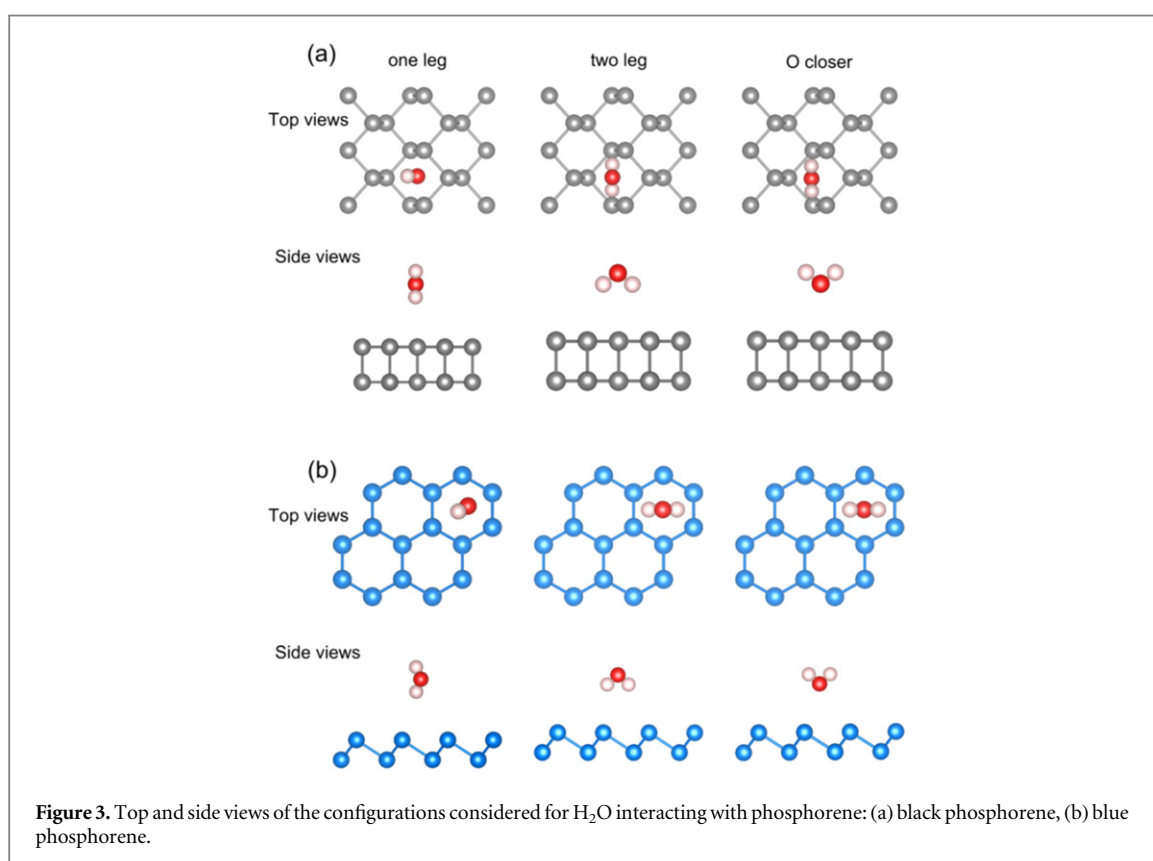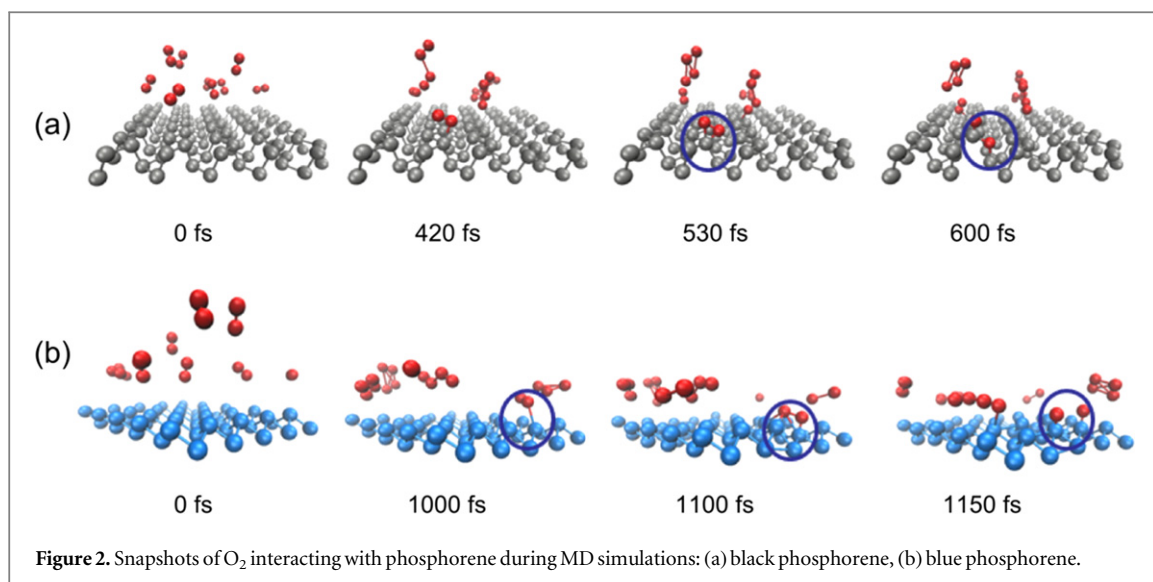
(i) The 'two leg' configuration is the most stable configuration suggesting that H atoms prefer to move towards the surface. This is due to the well-known polar nature of the H_2O molecule in which H atoms tend to attract the lone electron pairs of phosphorene.

(ii) The calculated binding energy which includes vdW correction term is about 180 and 125 meV for H_2O on the black and blue phosphorene, respectively. It is larger than that of H_2O on graphene at the same level of theory (in the range from 60 to 120 meV [32]), mainly because of the presence of the lone electron pairs on phosphorene. The attraction between H atoms and the lone electron pairs of phosphorene is clearly demonstrated by the deformation charge density plots (see figure S4 in the supplementary materials) showing the increase in the electron density in the region between H and P atoms.

In order to further examine the interaction of H_2O with phosphorene, we considered the initial configuration to consist of a 'forced' H_2O molecule at the interstitial site of the phosphorene lattice. If H_2O prefers to interact strongly with phosphorene, then the optimized configuration should show that H and O atoms remain in the lattice. This is not the case as H_2O moves out of the lattice to a surface site (figure S5 in the supplementary materials) without distorting the surface for both allotropes. Our first principles MD simulations up to 10 ps also find that H_2O molecules stay near the phosphorene surface without any chemical interaction within 10 ps (see video V5 in the supplementary materials). Therefore, H_2O prefers to bind to the surface through hydrogen bonds.

3.3. Stability of phosphorene in air : exposure to O_2 and H_2O

Based on the calculated results given in sections 3.1 and 3.2, we can state that the O_2 molecule could spontaneously dissociate on phosphorene at room temperature, and the H_2O molecule will not interact strongly with the pristine phosphorene.
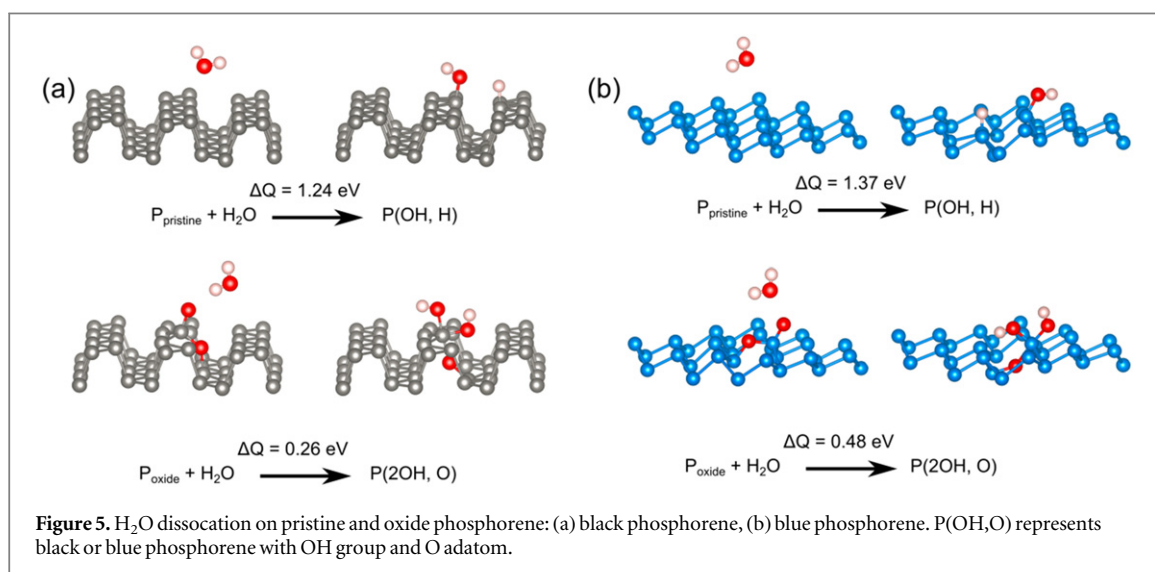
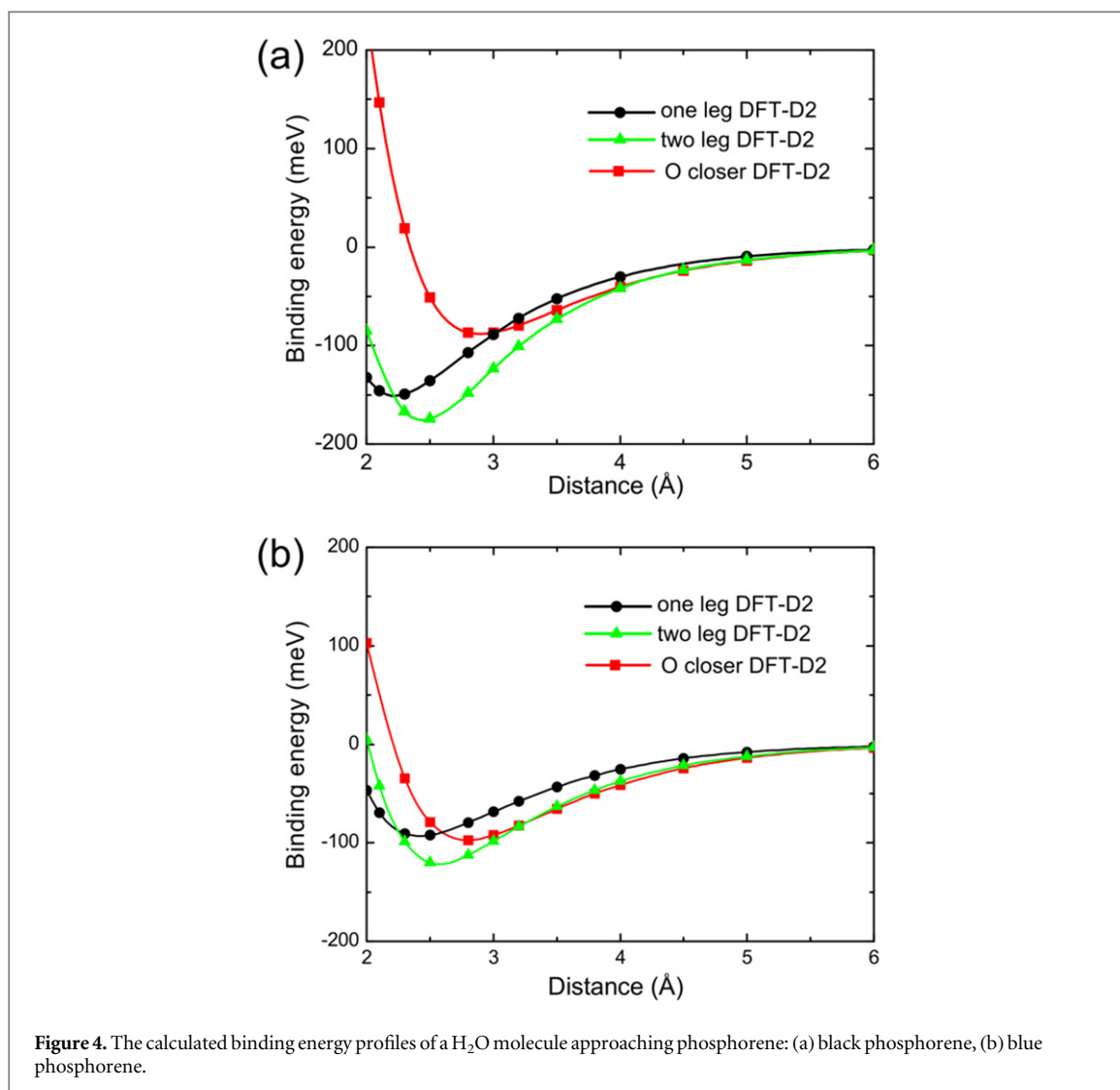The dissociation of H_2O on pristine black and blue phosphorene is endothermic with an energy increase of 1.24 eV and 1.37 eV, respectively (figure 5). This is not the case with the oxidized phosphorene monolayers for which the endothermic energy significantly decreases to 0.26 eV and 0.48 eV, respectively. Therefore, oxidation of phosphorene may enable dissociation of H_2O on the surface. Also considering that the

Figure 2. Snapshots of O_2 interacting with phosphorene during MD simulations: (a) black phosphorene, (b) blue phosphorene.

Figure 3. Top and side views of the configurations considered for H_2O interacting with phosphorene: (a) black phosphorene, (b) blue phosphorene.

phosphorous oxides (e.g., P_3O_6, P_4O_{10}) are reactive with H_2O [33], a simple intuitive view of the degradation of phosphorene in air based on energetic considerations can be offered: first, oxidation of the two-dimensional (2D) lattice of phosphorene will occur in air; then, the oxide species will interact with H_2O.
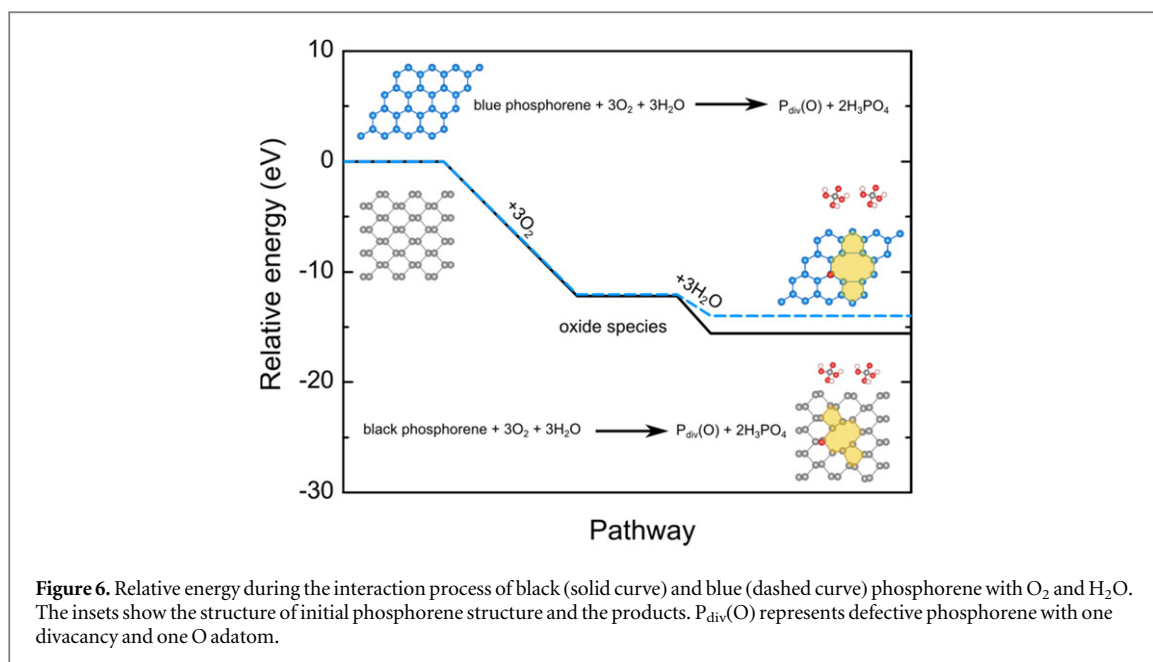
In order to validate our view of this interaction process, the relative energy of the initial and final chemical species along the pathway are calculated. The reactants are phosphorene, 3 O_2 molecules, and 3 H_2O molecules and the products are 2 phosphoric acid and phosphorene with defects including divacancy and O adatom (figure 6). For black phosphorene, the total energy release during this process is 15.60 eV. The oxidation process is exothermic with energy release of about 12.21 eV, and the reaction of phosphorene oxide species with 3 H_2O molecule further releases 3.39 eV of energy (see tables S2 and S3 in the supplementary materials for the details of the calculations). The reaction process for blue phosphorene is also exothermic, which suggests the similarity of black and blue phases in terms of the

Figure 4. The calculated binding energy profiles of a H_2O molecule approaching phosphorene: (a) black phosphorene, (b) blue phosphorene.

Figure 5. H_2O dissocation on pristine and oxide phosphorene: (a) black phosphorene, (b) blue phosphorene. P(OH,O) represents black or blue phosphorene with OH group and O adatom.

environmental stability. Overall, the exothermic process implies that H_2O will react with phosphorene if it is oxidized on the surface. The proposed pathway will lead to the formation of phosphoric acid and defective phosphorene. The defective phosphorene

could further be photo-oxidized [16], and then the oxide species will further react with H_2O. This reaction circle results in the fast degradation of phosphorene in air. The predicted mechanism for phosphorene is therefore different from the case of

Figure 6. Relative energy during the interaction process of black (solid curve) and blue (dashed curve) phosphorene with O_2 and H_2O. The insets show the structure of initial phosphorene structure and the products. $P_{div}(O)$ represents defective phosphorene with one divacancy and one O adatom.

graphene where the dangling bonds near the defect sites initiate its degradation [34].

4. Summary

In order to investigate the stability of phosphorene in air, interactions of O_2 and H_2O with phosphorene were studied by using DFT combined with first-principles MD simulations. We find that (i) O_2 will spontaneously dissociate on phosphorene at room temperature. The exposure of phosphorene to O_2 will induce its oxidation forming an oxidized phosphorene lattice; (ii) H_2O does not interact directly (chemically) with the pristine phosphorene lattice. It prefers to bind to the surface of phosphorene though hydrogen bonds; (iii) H_2O will exothermically interact with phosphorene if it has first been oxidized; (iv) other theoretically predicted 2D phosphorene allotropes, e.g. blue phosphorene, are also expected to be unstable in air.

Our calculations are supported by several experimental results; e.g. experiments have shown that fast degradation of phosphorene occurs in the presence of both O_2 and H_2O, the degradation process slows down with the exposure of phosphorene to only O_2 or H_2O [15, 35]; experiments have shown a drop of pH after water addition to phosphorene [13], which is a clear identification of the formation of phosphoric acid. Considering the rapid growth of research on 2D materials based on the group V semiconductors, our study provides an atomic scale understanding of the stability of phosphorene in air, which will aid in determining the degradation and aging effects of phosphorene-based devices.

References

[1] Li L, Yu Y, Ye G J, Ge Q, Ou X, Wu H, Feng D, Chen X H and Zhang Y 2014 Black phosphorus field-effect transistors *Nat. Nanotechnol.* **9** 372–7

[2] Liu H, Neal A T, Zhu Z, Luo Z, Xu X, Tománek D and Ye P D 2014 Phosphorene: an unexplored 2D semiconductor with a high hole mobility *ACS Nano* **8** 4033–41

[3] Wang G, Pandey R and Karna S P 2015 Atomically thin group V Elemental films: theoretical investigations of antimonene allotropes *ACS Appl. Mater. Interfaces* **7** 11490–6

[4] Zhiya Z, Jiafeng X, Dezheng Y, Yuhua W, Mingsu S and Desheng X 2015 Manifestation of unexpected semiconducting properties in few-layer orthorhombic arsenene *Appl. Phys. Express* **8** 055201

[5] Xia F, Wang H and Jia Y 2014 Rediscovering black phosphorus as an anisotropic layered material for optoelectronics and electronics *Nat. Commun.* **5** 4458

[6] Fei R and Yang L 2014 Strain-engineering the anisotropic electrical conductance of few-layer black phosphorus *Nano Lett.* **14** 2884–9

[7] Wood J D, Wells S A, Jariwala D, Chen K-S, Cho E, Sangwan V K, Liu X, Lauhon L J, Marks T J and Hersam M C 2014 Effective passivation of exfoliated black phosphorus transistors against ambient degradation *Nano Lett.* **14** 6964–70

[8] Andres C-G *et al* 2014 Isolation and characterization of few-layer black phosphorus *2D Mater.* **1** 025001

[9] Island J O, Steele G A, van der Zant H S and Castellanos-Gomez A 2015 Environmental instability of few-layer black phosphorus *2D Mater.* **2** 011002

[10] Koenig S P, Doganov R A, Schmidt H, Castro Neto A H and Özyilmaz B 2014 Electric field effect in ultrathin black phosphorus *Appl. Phys. Lett.* **104** 103106

[11] Buscema M, Groenendijk D J, Blanter S I, Steele G A, van der Zant H S J and Castellanos-Gomez A 2014 Fast and broadband photoresponse of few-layer black phosphorus field-effect transistors *Nano Lett.* **14** 3347–52

[12] Yau S-L, Moffat T P, Bard A J, Zhang Z and Lerner M M 1992 STM of the (010) surface of orthorhombic phosphorus *Chem. Phys. Lett.* **198** 383–8

[13] Hanlon D *et al* 2015 Liquid exfoliation of solvent-stabilized few-layer black phosphorus for applications beyond electronics *Nat. Commun.* **6** 8563

[14] Ziletti A, Carvalho A, Campbell D K, Coker D F and Castro Neto A H 2015 Oxygen defects in phosphorene *Phys. Rev. Lett.* **114** 046801

[15] Favron A, Gaufres E, Fossard F, Phaneuf-Lheureux A-L, Tang N Y W, Levesque P L, Loiseau A, Leonelli R, Francoeur S and Martel R 2015 Photooxidation and quantum confinement effects in exfoliated black phosphorus *Nat. Mater.* **14** 826–32

[16] Utt K L, Rivero P, Mehboudi M, Harriss E O, Borunda M F, Pacheco SanJuan A A and Barraza-Lopez S 2015 Intrinsic defects, fluctuations of the local shape, and the photo-oxidation of black phosphorus *ACS Cent. Sci.* **1** 320–7

[17] Sa B, Li Y-L, Qi J, Ahuja R and Sun Z 2014 Strain engineering for phosphorene: the potential application as a photocatalyst *J. Phys. Chem.* C **118** 26560–8

[18] Zhu Z and Tománek D 2014 Semiconducting layered blue phosphorus: a computational study *Phys. Rev. Lett.* **112** 176802

[19] Kresse G and Furthmüller J 1996 Efficiency of ab-initio total energy calculations for metals and semiconductors using a plane-wave basis set *Comput. Mater. Sci.* **6** 15–50

[20] Kresse G and Hafner J 1993 Ab initio molecular dynamics for open-shell transition metals *Phys. Rev.* B **48** 13115–8

[21] Perdew J P, Burke K and Ernzerhof M 1996 Generalized gradient approximation made simple *Phys. Rev. Lett.* **77** 3865–8

[22] Grimme S 2006 Semiempirical GGA—type density functional constructed with a long—range dispersion correction *J. Comput. Chem.* **27** 1787–99

[23] Nosé S 1984 A unified formulation of the constant temperature molecular dynamics methods *J. Chem. Phys.* **81** 511–9

[24] José M S, Emilio A, Julian D G, Alberto G, Javier J, Pablo O and Daniel S-P 2002 The SIESTA method for ab initio order- N materials simulation *J. Phys.: Condens. Matter* **14** 2745

[25] Newsome D A, Sengupta D, Foroutan H, Russo M F and van Duin A C 2012 Oxidation of silicon carbide by O2 and H_2O: a ReaxFF reactive molecular dynamics study: I *J. Phys. Chem.* C **116** 16111–21

[26] Zandiatashbar A, Lee G-H, An S J, Lee S, Mathew N, Terrones M, Hayashi T, Picu C R, Hone J and Koratkar N 2014 Effect of defects on the intrinsic strength and stiffness of graphene *Nat. Commun.* **5** 3186

[27] Kang J, Wood J D, Wells S A, Lee J-H, Liu X, Chen K-S and Hersam M C 2015 Solvent exfoliation of electronic-grade, two-dimensional black phosphorus *ACS Nano* **9** 3596–604

[28] Wang G, Pandey R and Karna S P 2015 Phosphorene oxide: stability and electronic properties of a novel two-dimensional material *Nanoscale* **7** 524–31

[29] Young D 2004 *Computational Chemistry: A Practical Guide for Applying Techniques to Real World Problems* (New York: Wiley)

[30] Wang G, Pandey R and Karna S P 2015 Effects of extrinsic point defects in phosphorene: B, C, N, O, and F adatoms *Appl. Phys. Lett.* **106** 173104

[31] Henkelman G, Arnaldsson A and Jónsson H 2006 A fast and robust algorithm for Bader decomposition of charge density *Comput. Mater. Sci.* **36** 354–60

[32] Ambrosetti A and Silvestrelli P L 2011 Adsorption of rare-gas atoms and water on graphite and graphene by van der Waals-corrected density functional theory *J. Phys. Chem.* C **115** 3695–702

[33] Twarowski A 1995 Reduction of a phosphorus oxide and acid reaction set *Combust. Flame* **102** 41–54

[34] Carlsson J M, Hanke F, Linic S and Scheffler M 2009 Two-step mechanism for low-temperature oxidation of vacancies in graphene *Phys. Rev. Lett.* **102** 166104

[35] Kuntz K L *et al* 2015 Understanding the effect of oxygen and water on 2D black phosphorus oxidation from photoelectron spectroscopy *Abstract in Int. Phosphorene Symp.* (*Lansing, USA*) (http://nanotube.pa.msu.edu/IPS15/IPS15abstracts.pdf)